

Chance-Constrained AC Optimal Power Flow – A Polynomial Chaos Approach

Tillmann Mühlpfordt,^a Line Roald,^b Veit Hagenmeyer,^a Timm Faulwasser,^a Sidhant Misra^c

Abstract—As the share of renewables in the grid increases, the operation of power systems becomes more challenging. The present paper proposes a method to formulate and solve chance-constrained optimal power flow while explicitly considering the full nonlinear AC power flow equations and stochastic uncertainties. We use polynomial chaos expansion to model the effects of arbitrary uncertainties of finite variance, which enables to predict and optimize the system state for a range of operating conditions. We apply chance constraints to limit the probability of violations of inequality constraints. Our method incorporates a more detailed and a more flexible description of both the controllable variables and the resulting system state than previous methods. Two case studies highlight the efficacy of the method, with a focus on satisfaction of the AC power flow equations and on the accurate computation of moments of all random variables.

Keywords—AC optimal power flow, uncertainty, polynomial chaos expansion, chance constraints

I. INTRODUCTION

The share of electricity generated through renewable energy sources such as wind and solar is increasing across the world [1]. This trend renders the operation of power systems more uncertain and more variable, which in turn has implications on all aspects of power systems operation—prompting a need for new and improved methods for uncertainty-aware scheduling and control. The present paper addresses the issue of modelling and mitigating the impact of uncertainty in optimal power flow (OPF) problems. These problems constitute an essential building block in power system operational processes such as market clearing [2] or security assessment [3]. Much of the existing literature has focused on modelling and solving stochastic optimization problems based on the DC power flow equations, including chance-constrained and robust versions of DC-OPF [4–8]. The increasing interest in using stochastic OPF in applications that require more detailed modelling of reactive power and voltage magnitudes, such as voltage control or distribution grid optimization, has inspired the development of methods that incorporate the full nonlinear AC power flow equations. Existing approaches include, e.g., chance constraints [9–14], robust formulations [15–18] OPF, and distributionally robust approaches [19]. The handling of the AC power flow constraints under stochastic nodal injections

is notoriously difficult, because (i) it requires propagating uncertainties through a set of implicit nonlinear equations; and (ii) algorithms that provide probabilistic or robust guarantees for constraint satisfaction often exploit convexity of the underlying optimization problem, which is not true for AC-OPF. The present paper addresses both of the above issues.

Existing methods have coped with these challenges differently. For example, [9, 12, 15, 16] use convex relaxations of the power flow constraints, allowing to use established stochastic optimization algorithms. Since the relaxations expand the feasible space, the solutions are however not guaranteed to be feasible for the original chance-constrained or robust AC-OPF problem. In [18], convex relaxations are used to provide a conservative estimate of the uncertainty impact, which guarantees robust constraint satisfaction, but sacrifices performance of the solution. The authors of [17] propose a robust AC-OPF based on convex inner approximations, however, the method requires controllable power injections at every node as it cannot satisfy the nodal power balance constraints with equality. Related approaches use a full or partial linearization of the AC power flow equations [13, 14], where the AC power flow constraints are linearized around an operating point and the problem is solved using methods similar to the approaches developed for the convex DC-OPF problem.

In the present paper we propose a tractable formulation of chance-constrained AC-OPF that essentially satisfies the full nonlinear AC power flow equations for generic uncertainties of finite variance, without relying on samples, relaxations or linearizations. Our problem formulation is based on polynomial chaos expansion (PCE), a spectral method for random variables analogous to a “Fourier series for random variables” [20]. Polynomial chaos allows to propagate uncertainty from the inputs to the relevant quantities such as current flows and voltage magnitudes, while accounting for the full nonlinearity of AC power flow. The accuracy of PCE-based problem formulations as well as the computational tractability depends on the maximum degree of the underlying polynomial basis. Theoretically, an infinite degree is required to satisfy the AC power flow equations *exactly*. However, we show by means of experiments that the AC power flow equations can be satisfied to high numerical accuracy for all uncertainty realizations already with low maximum degrees of about two or three. Furthermore, PCE facilitates moment-based reformulations of chance constraints, since the moments of all random variables can be computed directly from the PCE representation. In contrast to existing methods, PCE requires no linearization or sampling for either the moment computation or the chance-constrained formulation.

^aInstitute for Automation and Applied Informatics (IAI), Karlsruhe Institute of Technology (KIT), Karlsruhe, Germany, {tillmann.muehlpfordt, veit.hagenmeyer}@kit.edu, timm.faulwasser@ieee.org.

^bElectrical and Computer Engineering, University of Wisconsin - Madison, Madison, WI, USA, roald@wisc.edu.

^cLos Alamos National Laboratory, Los Alamos, NM, USA, sidhant@lanl.gov.

The primary advantage of PCE for stochastic OPF is its ability to accurately and efficiently handle *equality* constraints that involve random variables such as the full nonlinear AC power flow equations under uncertainty. At the same time PCE also helps enforcing *inequality* constraints using moment-based reformulations of chance constraints. While several alternatives have been explored in the literature to enforce inequality constraints under uncertainty—such as distributionally robust formulations where the uncertainty is modelled by a family of distributions that have matching (first two) moments [21]—structured methods that enforce equality constraints involving random variables remain less studied. For example, [13, 19] formulate chance-constrained and distributionally robust chance-constrained versions of the AC-OPF, but the AC power flow equations are satisfied only for the expected value while deviations are modelled through a linearization. Polynomial chaos allows a more elegant approach to AC power flow.

Polynomial chaos has been applied previously to power system optimization. For stochastic OPF under the DC approximation it has been shown that PCE provides exact and tractable convex reformulations [8, 22]. With AC equations, [23, 24] apply polynomial chaos to formulate the problem. However, [23] considers only constraints for the expected values of generated powers, and [24] does neither account for voltage magnitude constraints nor for line limits. Recently, PCE has been applied to the multi-period AC-OPF problem under uncertainty in [25]; a conic relaxation of the power flow equations is employed together with sparse regression to compute the PCE coefficients, based on the method from [23]. All works [23–25] lack a thorough probabilistic analysis of the satisfaction of the AC power flow equations, as well as a validation of the moments (mean and variance) of the power system state variables, such as line currents and bus voltages magnitudes. The present paper aims to close that gap. The contributions are as follows: (i) a framework to formulate chance-constrained AC-OPF using PCE as a one-shot optimization problem, accounting for voltage magnitude and current magnitude limits, but without relying on samples, relaxations or linearizations; (ii) investigation of AC power flow satisfaction for varying maximum degrees of the PCE basis; and (iii) validation of accuracy of moments, and comparison to linearized AC power flow. (iv) validation of empirical constraint satisfaction via in- and out-of-sample tests.

Paper organization: Section II discusses the power system model, the uncertainty model, and the chance-constrained OPF problem. Section III introduces PCE and its advantages for AC-OPF. Section IV applies PCE to chance-constrained OPF, and provides a tractable reformulation. The case studies (for a 5- and 30-bus system) from Section V demonstrate the efficacy of the proposed approach.

II. PROBLEM FORMULATION

A. Power System Model

Consider a connected N -bus electrical network represented by its set of bus indices $\mathcal{N} = \{1, \dots, N\}$, and its set of line indices $\mathcal{L} \subseteq \mathcal{N} \times \mathcal{N}$. At each bus $i \in \mathcal{N}$, we define the complex power $s_i = p_i + \text{j}q_i$, where p_i and q_i are the net active power

and reactive power respectively. The bus voltages are defined in rectangular coordinates, with v_i^{re} and v_i^{im} denoting the real and imaginary voltage components, respectively. The voltage magnitudes are given by $v_i = \sqrt{(v_i^{\text{re}})^2 + (v_i^{\text{im}})^2}$. In steady state the electrical network is governed by the nonlinear AC power flow equations, here given in rectangular form,

$$\begin{aligned} p_i &= \sum_{j \in \mathcal{N}} G_{ij}(v_i^{\text{re}}v_j^{\text{re}} + v_i^{\text{im}}v_j^{\text{im}}) + B_{ij}(v_i^{\text{im}}v_j^{\text{im}} - v_i^{\text{re}}v_j^{\text{re}}), \\ q_i &= \sum_{j \in \mathcal{N}} G_{ij}(v_i^{\text{im}}v_j^{\text{im}} - v_i^{\text{re}}v_j^{\text{re}}) - B_{ij}(v_i^{\text{re}}v_j^{\text{re}} + v_i^{\text{im}}v_j^{\text{im}}), \end{aligned} \quad (1)$$

for all buses $i \in \mathcal{N}$. The matrix $Y = G + \text{j}B \in \mathbb{C}^{N \times N}$ is the bus admittance matrix, which accounts for bus and line shunts as well as transformer tap ratios. For ease of presentation, the AC power flow equations (1) are written as a nonlinear system of algebraic equations $g : \mathbb{R}^{4N} \rightarrow \mathbb{R}^{2N}$

$$g(p, q, v^{\text{re}}, v^{\text{im}}) = 0. \quad (2)$$

In (2), the i th element of $p, q, v^{\text{re}}, v^{\text{im}} \in \mathbb{R}^N$ is $p_i, q_i, v_i^{\text{re}}, v_i^{\text{im}}$ for all buses $i \in \mathcal{N}$. For simplicity of notation, we assume each bus $i \in \mathcal{N}$ connects to one controllable generation unit p_i^{g} and one uncontrollable power injection p_i^{u} ,¹

$$p_i = p_i^{\text{g}} + p_i^{\text{u}}, \quad q_i = q_i^{\text{g}} + q_i^{\text{u}}, \quad \forall i \in \mathcal{N}. \quad (3)$$

B. Power System Model with Uncertainty

The power systems model (1)-(3) assumes a given and fixed set of power injections. However, power systems operation is influenced by uncertain factors such as fluctuations in temperature, wind speeds, or solar irradiation, which translate into uncertainty in system loading and renewable energy generation. In this paper, we differentiate between the exogenous drivers of the uncertainty, such as temperature or solar irradiation, and other random quantities that are functions of these exogenous drivers, such as load or solar PV production. The exogenous drivers are modelled through a generic random vector $\omega = [\omega_1, \dots, \omega_{N_\omega}]^T$ with $N_\omega \in \mathbb{N}$, and a corresponding set of possible realizations $\Omega \subset \mathbb{R}^{N_\omega}$. This random vector ω is referred to as the *stochastic germ*. To account for uncertainty in the AC power flow equations, the uncontrollable power injections p_i^{u} and/or q_i^{u} at bus $i \in \mathcal{N}$ are modelled as random variables that are (known) functions of the stochastic germ ω

$$p_i^{\text{u}} \triangleq p_i^{\text{u}}(\omega), \quad q_i^{\text{u}} \triangleq q_i^{\text{u}}(\omega), \quad \forall i \in \mathcal{N}. \quad (4a)$$

In our notation, sans-serif variables such as $p_i^{\text{u}}, q_i^{\text{u}}$ represent random variables. Realizations of these random variables for a given outcome $\omega \in \Omega$ are written as $p_i^{\text{u}}(\omega)$ or $q_i^{\text{u}}(\omega)$ to emphasize the functional dependency on the stochastic germ ω , although often $p^{\text{u}}, q^{\text{u}}$ will be used for compactness of notation. The size N_ω of the stochastic germ ω might be significantly lower than the size N of the uncertainties $p^{\text{u}}, q^{\text{u}}$. For example, consider temperature as a driver of load uncertainty: If a region is hit by a cold spell or a particularly hot day,

¹Multiple units at one bus can be easily handled by using matrices that map each generator or uncertainty source to their respective buses.

the variation in temperature tends to affect many loads in the region, albeit to different degrees.

In the following we assume that all occurring random variables have finite variance

$$\mathbb{V}[w_j], \mathbb{V}[p_i^u], \mathbb{V}[q_i^u] < \infty, \quad \forall j \in \{1, \dots, N_\omega\}, \forall i \in \mathcal{N}, \quad (4b)$$

where $\mathbb{V}[\cdot]$ denotes the variance. This assumption holds in the context of power systems operations, since all quantities are bounded by practical limits such as installed power capacity. The assumption (4b) allows us to handle fairly general cases without imposing any restrictive assumptions on the uncertainty distributions, for example Gaussian.

A consequence of the uncertainty model (4) is that *all* variables describing the network ($p, q, v^{\text{re}}, v^{\text{im}}$) become random vectors ($\mathbf{p}(\omega), \mathbf{q}(\omega), \mathbf{v}^{\text{re}}(\omega), \mathbf{v}^{\text{im}}(\omega)$). In other words, different realizations $\omega \in \Omega$ define different realizations of the uncertain injections ($p_i^u(\omega), q_i^u(\omega)$) according to the model (4). This again leads to different realizations of the net active/reactive powers ($p(\omega), q(\omega)$) and voltages ($v^{\text{re}}(\omega), v^{\text{im}}(\omega)$), consistent with the system behavior described by the AC power flow equations (2). Put differently, the uncertainties ($p^u(\omega), q^u(\omega)$) are propagated through the power flow equations (2)

$$\omega \stackrel{(4)}{\Rightarrow} (\mathbf{p}^u(\omega), \mathbf{q}^u(\omega)) \stackrel{(2)}{\Rightarrow} (\mathbf{p}(\omega), \mathbf{q}(\omega), \mathbf{v}^{\text{re}}(\omega), \mathbf{v}^{\text{im}}(\omega)). \quad (5)$$

Mathematically, the random variables from (5) are defined by the AC power flow

$$\forall \omega \in \Omega : \begin{cases} 0 = g(\mathbf{p}(\omega), \mathbf{q}(\omega), \mathbf{v}^{\text{re}}(\omega), \mathbf{v}^{\text{im}}(\omega)), & (6a) \\ \mathbf{p}(\omega) = \mathbf{p}^g(\omega) + \mathbf{p}^u(\omega), & (6b) \\ \mathbf{q}(\omega) = \mathbf{q}^g(\omega) + \mathbf{q}^u(\omega). & (6c) \end{cases}$$

The set of equations (6) can be interpreted as an algebraic equations on random variables. The formulation (6) requires the AC power flow equations to hold for arbitrary uncertainty realizations ω . The challenge of modelling the behavior of the nonlinear system and enforcing the AC power flow equations under uncertainty is a key aspect addressed in this paper.

C. Chance-constrained Optimal Power Flow

In our formulation the goal of chance-constrained OPF (CC-OPF) is to minimize the expected cost of generation, while satisfying the AC power flow equations for any realization of uncertainty and while guaranteeing that engineering constraints such as voltage magnitude and line current limits will hold up to a pre-specified probability, i.e.

$$\min_{\mathbf{p}_i^g, \mathbf{q}_i^g, \mathbf{v}_i^{\text{re}}, \mathbf{v}_i^{\text{im}}} \mathbb{E} \left[\sum_{i \in \mathcal{N}} f_i(\mathbf{p}_i^g) \right] \quad \text{subject to} \quad (7a)$$

$$g(\mathbf{p}, \mathbf{q}, \mathbf{v}^{\text{re}}, \mathbf{v}^{\text{im}}) = 0, \quad (7b)$$

$$\mathbf{p} = \mathbf{p}^g + \mathbf{p}^u, \quad \mathbf{q} = \mathbf{q}^g + \mathbf{q}^u, \quad (7c)$$

$$\mathbb{P}(x \geq x^{\text{min}}) \geq 1 - \varepsilon_x, \quad x \in \{\mathbf{p}_i^g, \mathbf{q}_i^g, \mathbf{v}_i\}, \quad (7d)$$

$$\mathbb{P}(x \leq x^{\text{max}}) \geq 1 - \varepsilon_x, \quad x \in \{\mathbf{p}_i^g, \mathbf{q}_i^g, \mathbf{v}_i\}, \quad (7e)$$

$$\mathbb{P}(i_{i-j} \leq i_{i-j}^{\text{max}}) \geq 1 - \varepsilon_i, \quad (7f)$$

$$\mathbf{v}_{i\theta V}^{\text{im}} = 0, \quad \forall i \in \mathcal{N}, \forall ij \in \mathcal{L}. \quad (7g)$$

Problem (7) minimizes the expected cost of active power generation (7a). Constraints (7b), (7c) are the power flow equations in terms of random variables, see (6); in other words, the AC power flow equalities hold for all realizations of the uncertainties. We consider technical limits on the generator active power p_i^g and reactive power q_i^g , as well as constraints on the voltage magnitudes v_i in (7d), (7e), and line current magnitudes i_{i-j} in (7f).² These constraints are enforced as *chance constraints* with respective acceptable violation probabilities $\varepsilon_p, \varepsilon_q, \varepsilon_v, \varepsilon_i \in [0, 1]$. The voltage angle reference is set to zero for all realizations of the uncertainty by (7g). An implicit assumption in this paper is that there exists a (high-voltage) solution of the power flow equations for all uncertainty realizations, and that (7b), (7c) models this (high-voltage) solution. Further, we observe that the generation dispatch will change as a function of the uncertainty realization, giving rise to an infinite number of variables in formulation (7). While we discuss how we obtain a finite dimensional representation of the optimization problem, the formulation applied in this paper does not assume any particular form of generator response. Specifically, it is not limited to, e.g., automatic generation control or other affine control policies common in the literature [4].

D. Solution Approach

In its present form Problem (7) seems intractable owing to infinite-dimensional decision variables, infinite-dimensional equality constraints, and chance constraints that are numerically challenging to evaluate. We tackle these challenges by expanding all random variables appearing in Problem (7), using a polynomial basis that is orthogonal with respect to the probability measure \mathbb{P} . This approach is called polynomial chaos expansion (PCE) [20, 26]. Polynomial chaos allows to reduce the infinite-dimensional constraints in (7) to a set of algebraic equations in the coefficients of the basis polynomials (so-called Galerkin projection [20, 26]). This way, the infinite-dimensional constraints can be satisfied up to arbitrary numerical accuracy by choosing an appropriately large degree of the polynomial basis, thus bypassing the need for linear approximations, restrictive assumptions on the uncertainty, and/or Monte-Carlo simulations. Furthermore, polynomial chaos also allows to compute moments of random variables efficiently without having to sample. Thus, it allows to formulate the tasks of uncertainty propagation, moment computation, and optimization elegantly as a single problem; i.e. we reformulate (7) as a one-shot finite-dimensional optimization problem.

III. INTRODUCTION TO POLYNOMIAL CHAOS EXPANSION

This section gives a brief overview of polynomial chaos expansion, focusing on its advantages for CC-OPF. Clearly, the here-given introduction to PCE is non-exhaustive; we refer to [20, 26] for a more detailed treatment.

²Based on the complex line current from line i to line j which is $i_{i-j} = y_{ij}(e_k - e_m) + jb_{ij}^{\text{sh}}e_i$ with the complex voltages e_i, e_j , branch admittance y_{ij} , and shunt susceptance b_{ij}^{sh} .

A. Polynomial Chaos Expansion

Polynomial chaos is a Hilbert space method for random variables that allows a structured representation of uncertainties in terms of deterministic, so-called PCE coefficients. Consider N_ω independent random variables ω_i of finite variance for $i = 1, \dots, N_\omega$. The random vector $\omega \cong [\omega_1, \dots, \omega_{N_\omega}]^\top$ is called the stochastic germ. Consider the N_ω -variate polynomials $\{\psi_k\}_{k=0}^\infty$ that are orthogonal with respect to the probability measure $\mathbb{P}(\omega)$, such that

$$\mathbb{E}[\psi_\ell \psi_k] = \langle \psi_\ell, \psi_k \rangle = \int \psi_\ell(\omega) \psi_k(\omega) d\mathbb{P}(\omega) = \gamma_\ell \delta_{\ell k}, \quad (8)$$

for all $\ell, k \in \mathbb{N}_0$. In (8) the scalar γ_ℓ is positive, and $\delta_{\ell k}$ is the Kronecker-delta. Notice that every polynomial $\psi_k = \psi_k(\omega)$ is itself a random variable. The orthogonal polynomials are indexed such that their degrees are non-decreasing. We define $\psi_0 = 1$ as the zero-order polynomial. Polynomial chaos expansion allows any real-valued random variable of finite variance that is a function of the stochastic germ ω to be expressed as a linear combination of the orthogonal polynomials $\{\psi_k\}_{k=0}^\infty$. Specifically, the PCE of the random variable \hat{x} is given by

$$\hat{x} = \sum_{k=0}^{\infty} x_k \psi_k \quad \text{with} \quad x_k = \frac{\langle \hat{x}, \psi_k \rangle}{\langle \psi_k, \psi_k \rangle} \in \mathbb{R}. \quad (9a)$$

The scalars x_k are the so-called PCE coefficients.³ For numerical implementations the infinite sum (9a) is truncated after $K+1 \in \mathbb{N}$ terms. In this case, we obtain an approximation x of the original random variable \hat{x} ,

$$\hat{x} \approx x = \sum_{k \in \mathcal{K}} x_k \psi_k \quad \text{with} \quad \mathcal{K} = \{0, \dots, K\}. \quad (10a)$$

The truncation error $\|\hat{x} - x\|$ is orthogonal to x and decays to zero for $K \rightarrow \infty$ in the induced norm $\|\cdot\|$, see [20, 26].

B. Uncertainty Propagation and Moment Computation

We describe how PCE can be used to (i) propagate uncertainties through (nonlinear) equations, and to (ii) compute moments of output variables.

1) *Uncertainty Propagation*: Consider a given random vector x that is mapped/propagated to the random vector y according to $h(x, y) = 0$. If the PCE coefficients x_k of x are known, the coefficients y_k of y can be determined by (intrusive) Galerkin projection; i.e. by projecting onto all orthogonal bases functions ψ_j [20, 26]

$$\begin{aligned} \forall j \in \mathcal{K} : 0 &= \left\langle h \left(\sum_{k \in \mathcal{K}} x_k \psi_k, \sum_{k \in \mathcal{K}} y_k \psi_k \right), \psi_j \right\rangle \\ &=: h_j(x_0, \dots, x_K, y_0, \dots, y_K). \end{aligned} \quad (11)$$

Hence, the Galerkin projection (11) allows to solve the stochastic problem $h(x, y) = 0$ by means of $(K+1)$ deterministic and tractable relations $h_j(\cdot)$. The projection error attains a minimum in the induced norm $\|\cdot\|$ and decays to zero for $K \rightarrow \infty$ [20, 26].

³For an \mathbb{R}^n -valued random vector z , the PCE representation is obtained by taking the PCE of every component, such that we obtain \mathbb{R}^n -valued vectors of PCE coefficients $z_k \in \mathbb{R}^n$.

2) *Computation of Moments*: The moments of a random variable x can be expressed as deterministic functions of the PCE coefficients x_k . For example, the expectation $\mathbb{E}[x]$ and the standard deviation $\sigma[x]$ are

$$\mathbb{E}[x] = x_0, \quad \sigma[x] = \mathbb{V}[x]^{1/2} = \left(\sum_{k \in \mathcal{K} \setminus \{0\}} \gamma_k x_k^2 \right)^{1/2}, \quad (12)$$

which follows from orthogonality of the basis according to (8).

C. Construction of Polynomial Basis

For each component ω_i of the stochastic germ ω , let $\{\psi_k^{(i)}\}_{k=0}^{N_d}$ be the univariate basis of orthogonal polynomials $\psi_k^{(i)}(\omega_i)$ with respect to $\mathbb{P}(\omega_i)$, with the degree of $\psi_k^{(i)}$ equal to k . Then the multivariate PCE basis with respect to the combined stochastic germ $\omega \cong [\omega_1, \dots, \omega_{N_\omega}]^\top$ of maximum degree N_d is given by

$$\{\psi_k\}_{k=0}^K \equiv \left\{ \prod_{i=1}^{N_\omega} \psi_{k_i}^{(i)} : 0 \leq \sum_i k_i \leq N_d \right\}. \quad (13)$$

Notice that the *dimension* of the multivariate basis $\{\psi_k\}_{k=0}^K$ is given by $K+1 = (N_\omega + N_d)! / (N_\omega! N_d!)$.

To better explain how a multivariate basis is constructed from a set of univariate bases, we provide a simple example.

Example 1 (Bivariate basis of degree at most 2). *Consider a bivariate stochastic germ ω with $N_\omega = 2$. For each ω_i let the respective univariate basis $\{\psi_k^{(i)}\}_{k=0}^{K_i}$ have degree $N_d = 2$, where $i \in \{1, 2\}$. Each univariate basis has dimension $K_i + 1 = 3$ such that $\{\psi_k^{(1)}\}_{k=0}^2 = \{1, \psi_1^{(1)}, \psi_2^{(1)}\}$, and $\{\psi_k^{(2)}\}_{k=0}^2 = \{1, \psi_1^{(2)}, \psi_2^{(2)}\}$, from which the bivariate basis of degree at most $N_d = 2$ is constructed as*

$$\underbrace{\{1\}}_{\text{deg}=0}, \underbrace{\{\psi_1^{(1)}, \psi_1^{(2)}\}}_{\text{deg}=1}, \underbrace{\{\psi_2^{(1)}, \psi_1^{(1)}\psi_1^{(2)}, \psi_2^{(2)}\}}_{\text{deg}=2} =: \{\psi_k\}_{k=0}^K.$$

Hence $K = 5$, which is in accordance with (13). \square

It is desirable to choose a PCE basis that allows an exact representation of a random variable at a low polynomial degree N_d , as the dimension $(K+1)$ —and hence the computational burden—grows rapidly with the degree N_d . For several univariate continuous random variables the corresponding orthogonal bases are well known and can be used off-the-shelf. For example, Hermite polynomials correspond to Gaussian distributions, Jacobi polynomials to Beta distributions, Laguerre polynomials to Gamma distributions [20]. These random variables admit an *exact* univariate PCE with a basis of maximum degree $N_d = 1$ in the respective bases of dimension $K+1 = 2$. In other words, random variables that follow Gaussian/Beta/Gamma distributions require only two PCE coefficients to be modelled *exactly*, i.e. there is no error in (10). In case the random variable is *not* Gaussian/Beta/Gamma, but reasonably similar, the respective bases may still be used at the expense of having to add higher-order coefficients. For arbitrary random variables of finite variance it is still possible to find the orthogonal basis such that two PCE coefficients suffice to model the uncertainty exactly.

Table I. REFORMULATIONS OF POWER FLOW EQUATIONS AND MOMENTS IN TERMS OF PCE COEFFICIENTS.

Rectangular power flow in terms of PCE coefficients with $i \in \mathcal{N}$, $k \in \mathcal{K}$
$\langle \psi_k, \psi_k \rangle (p_{i,k}^g - p_{i,k}^u) = \sum_{j \in \mathcal{N}} \sum_{k_1, k_2 \in \mathcal{K}} \langle \psi_{k_1} \psi_{k_2}, \psi_k \rangle (G_{ij}(v_{i,k_1}^{\text{re}} v_{j,k_2}^{\text{re}} + v_{i,k_1}^{\text{im}} v_{j,k_2}^{\text{im}}) + B_{ij}(v_{i,k_1}^{\text{im}} v_{j,k_2}^{\text{re}} - v_{i,k_1}^{\text{re}} v_{j,k_2}^{\text{im}}))$
$\langle \psi_k, \psi_k \rangle (q_{i,k}^g - q_{i,k}^u) = \sum_{j \in \mathcal{N}} \sum_{k_1, k_2 \in \mathcal{K}} \langle \psi_{k_1} \psi_{k_2}, \psi_k \rangle (G_{ij}(v_{i,k_1}^{\text{re}} v_{j,k_2}^{\text{re}} - v_{i,k_1}^{\text{re}} v_{j,k_2}^{\text{im}}) - B_{ij}(v_{i,k_1}^{\text{re}} v_{j,k_2}^{\text{re}} + v_{i,k_1}^{\text{im}} v_{j,k_2}^{\text{im}}))$
Moments of squared line current magnitudes with $ij \in \mathcal{L}$, $v_{ij,k}^{\text{re}} = v_{i,k}^{\text{re}} - v_{j,k}^{\text{re}}$, $v_{ij,k}^{\text{im}} = v_{i,k}^{\text{im}} - v_{j,k}^{\text{im}}$
$\mathbb{E}[i_{i-j}^2] = y_{ij}^{\text{br}} ^2 \sum_{k \in \mathcal{K}} \langle \psi_k, \psi_k \rangle ((v_{ij,k}^{\text{re}})^2 + (v_{ij,k}^{\text{im}})^2)$
$\sigma[i_{i-j}^2]^2 = y_{ij}^{\text{br}} ^4 \sum_{k_1, k_2, k_3, k_4 \in \mathcal{K}} \langle \psi_{k_1} \psi_{k_2} \psi_{k_3} \psi_{k_4} \rangle (v_{i,k_1}^{\text{re}} v_{ij,k_2}^{\text{re}} v_{i,k_3}^{\text{re}} v_{ij,k_4}^{\text{re}} + 2v_{i,k_1}^{\text{re}} v_{ij,k_2}^{\text{re}} v_{ij,k_3}^{\text{im}} v_{i,k_4}^{\text{im}} + v_{ij,k_1}^{\text{im}} v_{ij,k_2}^{\text{im}} v_{ij,k_3}^{\text{im}} v_{ij,k_4}^{\text{im}}) - \mathbb{E}[i_{i-j}^2]^2$
Moments of squared voltage magnitudes with $i \in \mathcal{N}$
$\mathbb{E}[v_i^2] = \sum_{k \in \mathcal{K}} \langle \psi_k, \psi_k \rangle ((v_{i,k}^{\text{re}})^2 + (v_{i,k}^{\text{im}})^2)$
$\sigma[v_i^2]^2 = \sum_{k_1, k_2, k_3, k_4 \in \mathcal{K}} \langle \psi_{k_1} \psi_{k_2} \psi_{k_3} \psi_{k_4} \rangle (v_{i,k_1}^{\text{re}} v_{i,k_2}^{\text{re}} v_{i,k_3}^{\text{re}} v_{i,k_4}^{\text{re}} + 2v_{i,k_1}^{\text{re}} v_{i,k_2}^{\text{re}} v_{i,k_3}^{\text{im}} v_{i,k_4}^{\text{im}} + v_{i,k_1}^{\text{im}} v_{i,k_2}^{\text{im}} v_{i,k_3}^{\text{im}} v_{i,k_4}^{\text{im}}) - \mathbb{E}[v_i^2]^2$

Mathematically, this amounts to constructing polynomials that are orthogonal with respect to the probability density that describes the uncertainty. This procedure is applicable to both discrete and continuous densities [26]. If the uncertainty is instead described in terms of samples (for example historical data samples), one can proceed by first fitting a density function to the data points. Subsequently, the basis can be constructed either through Gram-Schmidt orthogonalization, the Stieltjes procedure, or the Chebyshev algorithm [27].

IV. CHANCE-CONSTRAINED OPF USING PCE

Having introduced CC-OPF in Section II, and PCE in Section III, we now reformulate the CC-OPF Problem (7) as a one-shot optimization problem, namely Problem (22).

1) *Power Injection Uncertainty via PCE*: As seen in Section III, a continuous random variable can be represented in terms of its deterministic PCE coefficients. Given a polynomial basis $\{\psi_k\}_{k \in \mathcal{K}}$ with $\mathcal{K} = \{0, \dots, K\}$ that is orthogonal with respect to the probability measure $\mathbb{P}(\omega)$, we can represent the nodal power injection uncertainty from (4) by

$$p_i^u = \sum_{k \in \mathcal{K}} p_{i,k}^u \psi_k, \quad q_i^u = \sum_{k \in \mathcal{K}} q_{i,k}^u \psi_k \quad \forall i \in \mathcal{N}, \quad (14a)$$

where p^u, q^u may follow any distribution with finite variance.

2) *Uncertainty Propagation for AC Power Flow*: As described in Section II-A, uncertainty in power injections leads to all network variables $(p, q, v^{\text{re}}, v^{\text{im}})$ behaving as N -valued random vectors $(\mathbf{p}, \mathbf{q}, \mathbf{v}^{\text{re}}, \mathbf{v}^{\text{im}})$. We hence model all the network variables using PCE in a common multivariate basis,

$$\mathbf{x} = \sum_{k \in \mathcal{K}} x_k \psi_k \quad \forall \mathbf{x} \in \{\mathbf{p}_i, \mathbf{q}_i, \mathbf{v}_i^{\text{re}}, \mathbf{v}_i^{\text{im}}, \mathbf{p}_i^g, \mathbf{q}_i^g\}, \quad \forall i \in \mathcal{N}, \quad (15)$$

where x_k is the k th PCE coefficient of the variable \mathbf{x} , while the basis polynomials $\{\psi_k\}_{k \in \mathcal{K}}$ are the same for all variables. Characterizing all the network random variables involves uncertainty propagation through the nonlinear AC power flow equations, which is in general challenging. As described in Section III-B1 it is a main advantage of PCE that it allows to perform this task efficiently using Galerkin projection. The Galerkin projection (11) applied to the linear equality constraints (7c) and (7g) is straightforward,

$$p_k = p_k^g + p_k^u, \quad q_k = q_k^g + q_k^u, \quad v_{i\theta\nu,k}^{\text{im}} = 0, \quad \forall k \in \mathcal{K}. \quad (16)$$

Notice that the Galerkin projections (16) are *exact*, i.e., the projection errors are zero. Finally, Galerkin projection is applied

to the AC power flow equations (7b), following the approach in [23]. The resulting $2N(K+1)$ deterministic equations are listed in Table I. The Galerkin-projected power flow remains structurally equivalent to deterministic power flow from (1), i.e. the equations are quadratic in the real/imaginary parts of the bus voltages and their sparsity pattern is preserved. The scalar products $\langle \psi_{k_1} \psi_{k_2}, \psi_k \rangle$ from Table I can be computed offline using Gauss quadrature. As described in Section III-A, truncating the PCE at finite K incurs a truncation error.⁴ The error can be made as small as desired (see description below (10)) by increasing K at the cost of increased computational burden. However, as demonstrated in the case studies (Section V), low maximum degrees and hence low PCE dimensions suffice to satisfy the power flow equations to a practical level of accuracy.

3) *Cost Function*: We consider convex quadratic costs

$$f_i(\mathbf{p}_i^g) = c_{2,i}(\mathbf{p}_i^g)^2 + c_{1,i} \mathbf{p}_i^g, \quad (17)$$

with $c_{2,i} > 0$ for every bus $i \in \mathcal{N}$. The expected cost $\mathbb{E}[f_i(\mathbf{p}_i^g)]$ per bus from (7a) written in terms of PCE coefficients becomes

$$\mathbb{E}[f_i(\mathbf{p}_i^g)] = c_{2,i} \sum_{k \in \mathcal{K}} \gamma_k (p_{i,k}^g)^2 + c_{1,i} p_{i,0}^g =: \tilde{f}_i(p_{i,k}^g), \quad (18)$$

with $\gamma_k = \langle \psi_k, \psi_k \rangle$. Notice that the cost function $\tilde{f}_i(p_{i,k}^g)$ remains quadratic, but with respect to the PCE coefficients.

4) *Chance Constraint Representation*: We reformulate the chance constraints (7d)-(7f) based on information about their first two moments [13, 28, 29]. For example, the generation constraint in (7d) becomes

$$p_{g,i}^{\text{min}} \leq \mathbb{E}[p_i^g] \pm \lambda(\varepsilon_p) \sqrt{\mathbb{V}[p_i^g]} \leq p_{g,i}^{\text{max}}, \quad (19)$$

where $\lambda(\varepsilon_p) > 0$ is chosen based on knowledge about the random variable p_i^g . For example, in case p_i^g is Gaussian, the reformulation (19) is exact with $\lambda(\varepsilon_p) = \lambda_\Phi(\varepsilon_p) := \Phi^{-1}(1-\varepsilon_p)$, where $\Phi(\cdot)$ is the cumulative distribution function of a standard Gaussian [5, 6]. Owing to the nonlinearity of the AC power flow, the resulting propagated random variables for CC-OPF (7) are, however, non-Gaussian in general. Regardless, the distribution of those variables is often close to a Gaussian in practice. This is due to a concentration phenomenon similar to the central limit theorem [28, 30], making λ_Φ a good heuristic that we employ in the following [13]. In case the Gaussian heuristic is unsatisfactory, other choices of λ can

⁴ This error is not related to any approximation of the AC power flow. It stems from the finite truncation of the employed PCE basis.

be used to enforce so-called distributionally robust chance constraints that hold for a family of probability distributions rather than one specific distribution. As these choices require weaker assumptions (such as symmetry and/or unimodality of the distribution) they become more conservative [28, 29]. Alternatively, the parameter λ can be chosen numerically via cross-validation or through online adaptive methods [31].

The moment-based reformulation (19) is particularly suitable with PCE as moments can be directly obtained from the PCE coefficients, see (12). Thus, constraint (19) becomes

$$p_{g,i}^{\min} \leq p_{i,0}^g \pm \lambda(\varepsilon_p) \sqrt{\sum_{k \in \mathcal{K} \setminus \{0\}} \gamma_k (p_{i,k}^g)^2} \leq p_{g,i}^{\max}. \quad (20)$$

The reformulation of the other chance constraints for the generator reactive powers (7d)/(7e) follows the same procedure. The chance constraints for voltage magnitudes v_i (7d)/(7e) and line current magnitudes i_{i-j} (7f) are replaced by constraints on their squared magnitudes and the corresponding first and second moment. The magnitude chance constraints become

$$(v_i^{\min})^2 \leq \mathbb{E}[v_i^2] \pm \lambda(\varepsilon_v) \sqrt{\mathbb{V}[v_i^2]} \leq (v_i^{\max})^2, \quad (21a)$$

$$\mathbb{E}[i_{i-j}^2] + \lambda(\varepsilon_i) \sqrt{\mathbb{V}[i_{i-j}^2]} \leq (i_{i-j}^{\max})^2. \quad (21b)$$

The expressions for the moments are given in Table I. The reason for using the moment-based reformulation on v_i^2 and i_{i-j}^2 instead of v_i and i_{i-j} is that for the former, the moments can be obtained directly as an analytic function of the moments of v^{re} and v^{im} (Table I), whereas for the latter, obtaining the moments will require additional equality constraints.

5) *Tractable Reformulation*: The reformulations (15)-(21) allow to cast the chance-constrained OPF (7) as a finite-dimensional nonlinear program (NLP) with the PCE coefficients as decision variables

$$\min_{p_{i,k}^g, q_{i,k}^g, v_{i,k}^{\text{re}}, v_{i,k}^{\text{im}}} \sum_{i \in \mathcal{N}} \tilde{f}_i(p_{i,k}^g) \quad \text{subject to} \quad (22a)$$

Galerkin-projected power flow from Table I, (22b)

$$p_{g,i}^{\min} \leq p_{i,0} \pm \lambda(\varepsilon_p) \sigma[p_{i,k}^g] \leq p_{g,i}^{\max}, \quad (22c)$$

$$q_{g,i}^{\min} \leq q_{i,0} \pm \lambda(\varepsilon_q) \sigma[q_{i,k}^g] \leq q_{g,i}^{\max}, \quad (22d)$$

$$(v_i^{\min})^2 \leq \mathbb{E}[v_i^2] \pm \lambda(\varepsilon_v) \sigma[v_{i,k}^2] \leq (v_i^{\max})^2, \quad (22e)$$

$$\mathbb{E}[i_{ij}^2] + \lambda(\varepsilon_i) \sigma[i_{ij}^2] \leq (i_{i-j}^{\max})^2, \quad (22f)$$

$$v_{i\theta V,k}^{\text{im}} = 0, \quad \forall k \in \mathcal{K}, \forall i \in \mathcal{N}, \forall ij \in \mathcal{L}. \quad (22g)$$

The solution to Problem (22) allows for straightforward a-posteriori uncertainty propagation by means of a simple function evaluation, see (5)). This can be used, e.g. to determine appropriate generator set-points. That is, let ω be the realization of the uncertainty, then with PCE a-posteriori uncertainty propagation (5) becomes

$$\omega \Rightarrow \sum_{k \in \mathcal{K}} (p_k^u, q_k^u) \psi_k(\omega) \Rightarrow \sum_{k \in \mathcal{K}} (p_k^*, q_k^*, v_k^{\text{re}*}, v_k^{\text{im}*}) \psi_k(\omega) \quad (23)$$

where the superscript $(\cdot)^*$ denotes the solution to (22). To evaluate (23) means to evaluate the basis polynomials ψ_k at the realization ω , and then to multiply by the PCE coefficients—which is computationally cheap.

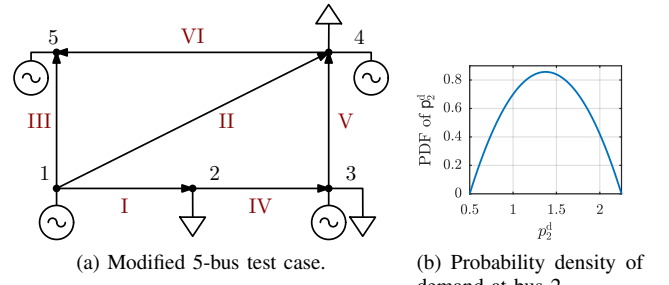


Figure 1. 5-bus test case and uncertainty model.

Bus i	$c_{2,i}$	$c_{1,i}$	$p_{g,i}^{\max}$	$q_{g,i}^{\max}$	v_i^{\min}	v_i^{\max}	Line $i-j$	i_{i-j}^{\max}
1	14	2	1.5	1.275	0.9	1.1	1-2	1.04
2	-	-	-	-	0.9	1.1	1-5	0.87
3	11	3	4.3	3.9	0.9	1.1	2-3	0.78
4	14	4	9.9	1.5	0.9	1.1		
5	13	1	1.5	4.5	0.9	1.1		

V. CASE STUDIES

Next, we demonstrate the practicability and advantages of PCE for stochastic optimal power flow. In particular we study the numerical accuracy of the AC power flow equations for varying maximum degrees; the accuracy of the moments; the empirical violation probability of selected inequality constraints both for in-sample and out-of-sample tests; and the shape of the generation policies.

In the case studies all numbers are given in per-unit (p.u.) for a base MVA of 100. Simulations were carried out on a standard desktop computer with 16 GB RAM and an i7-4770 CPU, and implemented in Julia using JuMP with Ipopt as NLP solver. We initialized the NLP (22) as follows. The zero-order PCE coefficients were set equal to the solution of the deterministic OPF problem with the uncertainties set to their expected values, while the higher-order coefficients were set to zero. The solution of the deterministic OPF also provided an initial guess for the active set of (22). To improve computational tractability, we applied a constraint generation method to solve the NLP. First, we solve the NLP including only the constraints that were active for the deterministic problem. Second, we check a posteriori whether the obtained solution satisfies *all* constraints. If a constraint is violated, we add the violated constraint to the problem, and solve the NLP again.

A. Satisfaction of AC Power Flow Constraints

As described in Section IV-2, there is a trade-off between the accuracy of AC power flow satisfaction and the PCE dimension $(K+1)$, which dictates the computational complexity. Since keeping the order K low is desirable, we investigate what is the smallest PCE degree that is sufficient for the AC power flow constraints to be satisfied up to a practical level of accuracy. These tests are performed on the 5-bus and 30-bus test case.

1) *5-Bus Test Case*: We consider a modified version of the 5-bus test from [32], shown in Figure 1a. We neglect the shunt elements, consider a quadratic cost function, and assume that the voltage magnitude at the slack bus 4 is constant at one. The

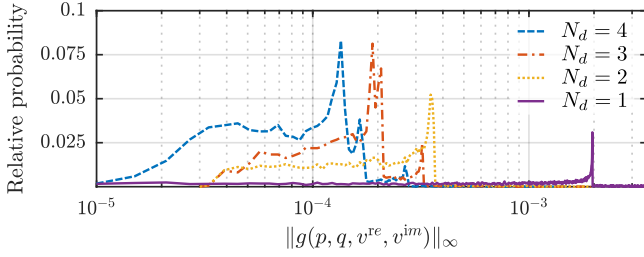


Figure 2. Relative probability of maximum AC power flow violation for polynomial bases of degree at most $N_d \in \{1, 2, 3, 4\}$ for 5-bus system.

line current limits are set equal to the per-unit MVA ratings. Other relevant parameters are summarized in Table II.

The active power demand at bus 2 is uncertain and follows a Beta distribution with support $[l, u] = [0.50, 2.25]$ and shape parameters $(\alpha, \beta) = (2, 2)$, $p_2^u = -p_2^d$ with $p_2^d \sim \text{B}([0.50, 2.25], 2, 2)$, with $\mathbb{E}[p_2^d] = 1.375$ and $\sigma[p_2^d] = 0.391$. The PCE coefficients are $[p_{2,0}^u, p_{2,1}^u] = 1/(\alpha+\beta) [\beta u + \alpha l, u-l]$. The probability density function is plotted in Figure 1b. Since the uncertainty is one-dimensional, the stochastic germ is equal to $\omega \sim \text{B}([0, 1], 2, 2)$, and the Jacobi polynomials provide the corresponding orthogonal basis [20]. For the chance constraints, we enforce $\varepsilon = \varepsilon_p = \varepsilon_q = \varepsilon_v = \varepsilon_i = 0.1$, and we set the inequality constraint parameter to $\lambda(\varepsilon) = \lambda_\Phi(\varepsilon) = 1.2816$, see Section IV-4.

We consider a single univariate source of uncertainty. Hence, the dimension and the maximum degree of the basis are linked by $K+1 = N_d+1$, implying that the number of constraints grows linearly with the maximum degree N_d . We draw 10 000 realizations of the uncertainty, and for each realization we compute the values of all remaining variables based on (23). To quantify the error in the AC power flow satisfaction, we compute the ∞ -norm of (2) for these realizations, and compare it against its ideal value of zero. The relative probability of $\|g(\cdot)\|_\infty$ is shown in Figure 2, where the different lines correspond to different maximum degrees N_d of the polynomial basis. As expected, a larger maximum degree N_d —hence a larger PCE dimension—leads to lower maximum AC power flow violations. There is a sharp decrease in the power flow inaccuracies from $N_d = 1$, with errors between $1 \text{ E-}3$ and $2 \text{ E-}3$, to $N_d = 2$ with errors approximately at $4 \text{ E-}4$. Further increases in the degree decrease the error even more, but not considerably. The order of PCE necessary for sufficient accuracy depends on the effective nonlinearity in the power flow equations. For example, in case of DC power flow, it is known that PCE with degree $N_d = 1$ is exact [8]. The fact that in our experiments a PCE basis of degree 2 has a small error shows that a degree of 2 is enough to capture the level of nonlinearity of the AC power flow equations for typical levels of uncertainty. The solution times for the NLP (22) are 0.45 s, 0.84 s, 0.67 s, 2.6 s for maximum degrees 1, 2, 3, 4, respectively.

2) *30-bus Test Case*: We consider a modified version of the 30-bus test case [32]. The shunt elements are neglected for simplicity, and the voltage magnitude at slack bus 1 is assumed constant at one. The line current limits are set to the nominal values of the per-unit line ratings, except for two lines where

Table III. MAX. AC POWER FLOW VIOLATION FOR 30-BUS SYSTEM.

Maximum degree N_d	1	2	3
Maximum power flow violation	3.8548E-5	3.66973E-6	2.34221E-8
NLP time in seconds	0.6	10.6	239.2

the capacity is reduced from 16 to, $i_{15-23}^{\max} = 11$, and $i_{25-27}^{\max} = 12$. Reducing the capacity on those two lines makes for a more interesting case, as several line current limits become binding.

We introduce a stochastic germ ω comprised of four distinct sources of uncertainty, two Beta distributions (one symmetric, one non-symmetric) and two normal distributions as described in Table VI. The stochastic germ ω is used to represent load uncertainty at six buses $i \in \mathcal{U} = \{2, 3, 4, 24, 10, 21\}$, as listed in the last column of Table VI. For each bus $i \in \mathcal{U}$, the uncertain load is modelled as $p_i^u = -p_i^d$ with $\mathbb{E}[p_i^d] = p_i^{\text{d,nom}}$, $\sigma[p_i^d] = s \cdot p_i^{\text{d,nom}}$, where $p_i^{\text{d,nom}}$ is the nominal value of the active power demand taken from the case file [32], and the relative standard deviation $s > 0$ describes the standard deviation as a fraction of the nominal load.

First, we fix the relative standard deviation $s = 0.15$ and the risk level $\varepsilon = 0.15$. We verify the satisfaction of the power flow equations for varying maximum degrees $N_d \in \{1, 2, 3\}$, according to the procedure from the 5-bus test case. Due to space constraints we provide only the maximum power flow violation across all samples in Table III. Graphically this corresponds to the right-most value in Figure 2 of every plotted line. Table III supports the findings from the 5-bus system—increasing the degree leads to higher accuracy of the power flow equations and degree 2 provides sufficient accuracy in practice. Notice that overall the power flow equations are more accurate for the 30-bus system compared to the 5-bus system. As the 5-bus system is more meshed, the effect of the uncertainty is greater there—even though there is just a single source of uncertainty.

B. In-sample Tests

In this section we investigate the capability of PCE to reduce the constraint violation probability to below an acceptable level. Since our chance constraint reformulation is based on the first and second moments of the uncertainty, we first assess their accuracy when computed with PCE. We then assess the ability of the method to limit the level of constraint violations.

1) *Accuracy of Moment Computation*: The quality of the moments is essential for the reformulations of the chance constraints, which is evident from (19) and (21). We compare the accuracy of the PCE-based moments with moments obtained from the full nonlinear AC power flow equations, and a linearized version of the AC power flow equations used in the literature [13]. The variables in the AC power flow equations are divided into *independent* variables—real and imaginary voltage at the slack bus, active power and voltage magnitude at the PV buses and real and reactive power injection at the PQ buses—and *dependent* variables, which consist of the rest. Each realization of the uncertainty ω fully specifies the *independent* variables: the real and reactive power consumption of the uncertain loads are determined by ω , and the active power and voltage magnitude at the PV buses are adjusted according to the control policy given by (23).

Table IV. ERROR IN THE COMPUTED MOMENTS FOR THE PCE METHOD (PCE) AND THE LINEARIZATION METHOD (LIN) FOR 30-BUS SYSTEM.

AC vs.	s	$\ \Delta\mu\ _\infty$	$\ \Delta\sigma\ _\infty$	$\ \Delta\mu\ _\infty$	$\ \Delta\sigma\ _\infty$	$\ \Delta\mu\ _\infty$	$\ \Delta\sigma\ _\infty$	$\ \Delta\mu\ _\infty$	$\ \Delta\sigma\ _\infty$
PCE	0.05	1.8 E-5	0.6 E-5	1.7 E-5	0.7 E-5	0.3 E-5	0.4 E-5	5.1 E-5	3.9 E-5
	0.10	10.1 E-5	0.4 E-5	2.0 E-5	2.0 E-5	2.2 E-5	1.0 E-5	33.4 E-5	5.7 E-5
	0.15	2.9 E-5	19.8 E-5	10.7 E-5	6.4 E-5	3.8 E-5	1.1 E-5	19.3 E-5	12.1 E-5
lin. AC	0.05	431.2 E-5	4.0 E-5	0.131	81.1 E-5	108.4 E-5	2.3 E-5	4901.5 E-5	104.0 E-5
	0.10	411.0 E-5	12.9 E-5	0.136	294.3 E-5	105.8 E-5	7.5 E-5	4812.1 E-5	196.3 E-5
	0.15	387.6 E-5	7.0 E-5	0.146	700.3 E-5	101.8 E-5	17.1 E-5	4715.7 E-5	348.1 E-5
Reference		$\ \mathbb{E}[p^g]_{AC}\ _\infty$ 0.5800	$\ \sigma[p^g]_{AC}\ _\infty$ 0.1132	$\ \mathbb{E}[q^g]_{AC}\ _\infty$ 0.3829	$\ \sigma[q^g]_{AC}\ _\infty$ 0.0038	$\ \mathbb{E}[v]_{AC}\ _\infty$ 1.0792	$\ \sigma[v]_{AC}\ _\infty$ 0.0012	$\ \mathbb{E}[i_{i-j}]_{AC}\ _\infty$ 0.3951	$\ \sigma[i_{i-j}]_{AC}\ _\infty$ 0.0100

Table V. EMPIRICAL CONSTRAINT SATISFACTION, COST, AND EXPECTED POWER FLOW VIOLATION FOR MAX. DEGREE $N_d \in \{1, 2\}$ FOR 30-BUS SYSTEM.

s	ε	Maximum degree $N_d = 1$							Maximum degree $N_d = 2$						
		$p_{g,3}^{\max}$	$p_{g,4}^{\max}$	i_{21-22}^{\max}	i_{15-23}^{\max}	i_{25-27}^{\max}	Cost	PF violation $\mathbb{E}[\cdot]/1 \text{ E-3}$	$p_{g,3}^{\max}$	$p_{g,4}^{\max}$	i_{21-22}^{\max}	i_{15-23}^{\max}	i_{25-27}^{\max}	Cost	PF violation $\mathbb{E}[\cdot]/1 \text{ E-3}$
0.10	0.05	0.9495	0.9499	0.9436	0.9514	0.9490	599.25	0.0640	0.9494	0.9499	0.9424	0.9526	0.9483	599.25	0.0009
	0.10	0.9026	0.9015	0.8954	0.8959	0.8980	599.24	0.0618	0.9022	0.9012	0.8953	0.8961	0.8980	599.24	0.0007
	0.15	0.8514	0.8507	0.8812	0.8515	0.8489	599.24	0.0601	0.8515	0.8506	0.8808	0.8516	0.8487	599.24	0.0006
0.15	0.05	0.9494	0.9499	0.9388	0.9486	0.9475	599.38	0.1502	0.9494	0.9500	0.9381	0.9511	0.9473	599.38	0.0042
	0.10	0.9028	0.9015	0.8938	0.8937	0.8969	599.36	0.1421	0.9030	0.9015	0.8927	0.8941	0.8969	599.36	0.0029
	0.15	0.8514	0.8502	0.8488	0.8427	0.8486	599.35	0.1373	0.8515	0.8501	0.8484	0.8426	0.8485	599.35	0.0024

Table VI. STOCHASTIC GERM AND AFFECTED BUSES.

ω_j	Distribution	Polynomial basis	Affected buses
1	B([0, 1], 2, 2)	Jacobi	2, 3
2	B([0, 1], 2, 5)	Jacobi	4
3	N(0, 1)	Hermite	24
4	N(0, 1)	Hermite	10, 21

For the 30-bus test case and a maximum degree of $N_d = 2$, we compare three sets of moments: (i) The PCE moments ($\mathbb{E}[\cdot]_{\text{PCE}}, \sigma[\cdot]_{\text{PCE}}$) obtained directly from (12). (ii) The moments for full AC power flow ($\mathbb{E}[\cdot]_{\text{AC}}, \sigma[\cdot]_{\text{AC}}$) obtained by drawing uncertainty samples, determining the value of the *independent* variables in a similar fashion as for PCE, and then solving the full AC equations to determine the value of the *dependent* variables. (iii) The moments of the linearized AC power flow ($\mathbb{E}[\cdot]_{\text{lin}}, \sigma[\cdot]_{\text{lin}}$) obtained via sampling, but the *dependent* variables are determined using a first-order Taylor approximation around the operating point corresponding to $\mathbb{E}[\omega]$.

If sufficiently many samples are used in the Monte Carlo simulations, the moments obtained from the full AC equations ($\mathbb{E}[\cdot]_{\text{AC}}, \sigma[\cdot]_{\text{AC}}$) can be considered as ground truth. The quality of the PCE and linearization is given by the ∞ -norm of the error relative to the AC solution. For the active power we compute the error by comparing the expected value via PCE to the expected value via the full AC power flow as

$$\|\Delta\mu\|_\infty = \|\mathbb{E}[p^g]_{\text{AC}} - \mathbb{E}[p^g]_{\text{PCE}}\|_\infty. \quad (24)$$

The error in the standard deviation σ for the PCE method, as well as the expected value and standard deviation for the linearization method are evaluated analogously.

Table IV summarizes the results for varying relative standard deviations s of the load, and for a total of 10000 Monte Carlo samples of the full AC power flow. We observe that PCE performs significantly better than the linearized power flow, with PCE giving errors that are orders of magnitude smaller. We observe that PCE errors ($\approx 1 \text{ E-5}$) are also small relative to the reference values in the last row of Table IV, implying that PCE is quite accurate for all considered values of the relative standard deviation s . Table IV also shows that the reactive power behaves more nonlinearly than the active

power, leading to larger errors in the reactive power estimation for the linearized power flow. Particularly the mean values are poorly estimated. Since the accuracy of the reformulated chance constraints requires accuracy in both mean and standard deviation, PCE is expected to be superior in enforcing chance constraints compared to the linearized AC power flow.

2) *Chance Constraint Satisfaction*: Next, we investigate how the maximum degree N_d affects constraint satisfaction. Table V summarizes the results for maximum degrees $N_d \in \{1, 2\}$, considering relative standard deviations $s \in \{0.10, 0.15\}$ and violation probabilities $\varepsilon \in \{0.05, 0.10, 0.15\}$. The empirical constraint satisfaction is computed from 10000 samples, evaluated using the full AC power flow equations. From Table V we observe that for both $N_d = 1$ and $N_d = 2$ there are no significant violations of the chance constraints, i.e., the empirical constraint satisfaction is close to the specified level $1 - \varepsilon$. There are several smaller inaccuracies in the enforcement of the chance constraints that may be attributed to the uncertainty being non-Gaussian, however, this effect appears to be small. The empirical constraint satisfaction for the two maximum degrees $N_d = 1$ and $N_d = 2$ is similar, although $N_d = 1$ yields slightly lower constraint satisfaction compared to $N_d = 2$. This may be because for $N_d = 1$ we are not able to capture the skewness of the distributions as well as for a maximum degree $N_d = 2$. Table V also shows the expected power flow (PF) violation. Consistent with our results in Section V-A, the expected power flow violation for the maximum degree $N_d = 1$ is considerably larger compared to $N_d = 2$, e.g. 0.1502 E-3 vs. 0.0042 E-3 for the relative standard deviation $s = 0.15$ and the violation probability $\varepsilon = 0.05$. To summarize, a higher maximum degree N_d ensures more accurate satisfaction of the power flow equations *and* of the chance constraints.

C. Out-of-sample Tests

Since it is frequently hard to obtain accurate estimates of the probability distributions in practical applications, we are also interested in understanding the out-of-sample performance of the method. To assess the out-of-sample performance, we test

the solution of (22) against distributions that are different from what we assumed when solving (22). In the following, we will refer to the uncertainty assumed within (22) as *modelled uncertainty*, and the uncertainty we test against as *actual uncertainty*.

We compute the solution of (22) for the stochastic germ from Table VI with a relative standard deviation $s = 0.15$ and a risk level $\varepsilon = 0.15$, and for varying maximum degrees $N_d \in \{1, 2, 3\}$. Each of these three solutions—which have the same modelled uncertainty but vary in the maximum polynomial degree—is stored and tested against two different actual uncertainties with respect to AC power flow and chance constraint satisfaction.

1) *Correct Distribution – Inaccurate Standard Deviations:* First, we perform out-of-sample test where the actual uncertainty belong to the same family of distributions as the modelled uncertainty (see Table VI), but where we have an inaccurate estimate of the standard deviations. In this case, the actual uncertainties still follow Beta and Normal distributions, but we scale the relative standard deviation of the actual uncertainty, such that we have three standard deviations $\{0.5s, s, 1.5s\}$, which are smaller, the same and larger than the assumed standard deviation. We include the case for which the actual uncertainty is equivalent to the modelled uncertainty to have a means of comparison.

The left plot of Figure 3 shows the maximum power flow violation among 10 000 samples for varying maximum degrees $N_d \in \{1, 2, 3\}$ as a function of the relative standard deviation s . For the same value of the relative standard deviation s the AC power flow satisfaction reduces greatly as the maximum degree increases. This is consistent with the results from Section V-A. On the other hand, the accuracy of the power flow equations appears fairly insensitive to inaccuracies in the standard deviation s . For example, for the maximum degree $N_d = 2$ the maximum power flow error is in the range of $1 \text{ E-}6$ for all values of the relative standard deviation s .

The variation of the empirical chance constraint satisfaction for different standard deviations is shown in the right plot of Figure 3 for the upper branch flow limit of the line connecting buses 21 and 22. We observe that empirical constraint satisfaction decreases with increasing values of s . Conversely, the constraint satisfaction appears is not dependent on the maximum degree N_d . It is not surprising that the empirical violation probability is sensitive to the inaccuracies in standard deviations, as the standard deviation enters directly into the expressions for the reformulated chance constraints. The increase in constraint satisfaction to more than 95% for $0.5s$ stems from the smaller support of the actual uncertainty relative to the modelled one.⁵ On the other hand, positive perturbations such as $1.5s$ increase the support beyond what was assumed in the reformulation, hence constraint violations are more frequent.

2) *Inaccurate Distributions – Correct Standard Deviation:* In our second set of experiments, the actual uncertainty

⁵Technically, the support is only smaller for the Beta distribution while it remains the real axis for Gaussians regardless of ν , but numerically the samples for the Gaussian distributions will have a smaller support.

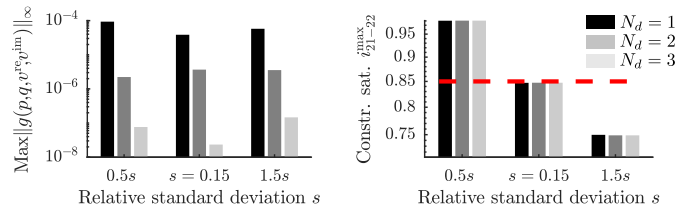


Figure 3. Correct distribution, inaccurate standard deviations – power flow violation and constraint satisfaction for varying maximum degrees.

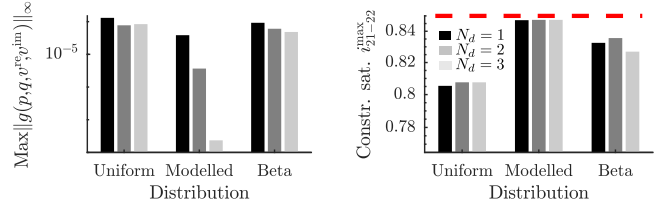


Figure 4. Inaccurate distributions, correct standard deviation – power flow violation and constraint satisfaction for varying maximum degrees.

matches the first two moments of the modelled uncertainty, but the underlying family of distributions is different. Specifically, the stochastic germ for the actual uncertainties is set to the uniform distribution $\omega_j \sim \mathcal{U}([0, 1])$ for $j \in \{1, 2, 3, 4\}$ in the first experiment, and to the Beta distribution $\omega_j \sim \mathcal{B}([0, 1], \alpha, \beta)$ with shape parameters $\alpha = \beta = 3$ for $j \in \{1, 2, 3, 4\}$ in the second experiment. Both of these cases are compared to the case for which the actual uncertainty matches the modelled uncertainty.

The left plot of Figure 4 shows the maximum power flow violation for varying maximum degrees $N_d \in \{1, 2, 3\}$ for the three different actual uncertainties. The exactness of the AC power flow still decreases with increasing the maximum degree, but the decrease is not as significant as the decrease seen in Figure 3. The empirical constraint satisfaction, however, still seems fairly insensitive to the maximum degree, although the desired level of $1 - \varepsilon = 0.85\%$ is met only for the case in which actual and modelled uncertainty coincide.

Based on the in-sample and out-of-sample tests we draw the following conclusions: (i) Increasing the maximum degree N_d leads to more accurate AC power flow, with $N_d = 2$ giving a good trade-off between exactness and computational overhead. The accuracy remains sufficiently high even when the actual distribution is different from the modelled distribution. We also conclude that the accuracy is more sensitive to estimation errors related to the *family* of distribution rather than to the *parameters* of the distribution. (ii) The chance constraints are satisfied almost to the same extent irrespective of the maximum degree N_d . It is much less sensitive to the PCE degree than it is to errors in the estimated distribution.

D. Generation Policies

The solution to the PCE provides a generation control policy which can be evaluated for any realization of uncertainty to provide guidance on how to redispatch generators in a economically efficient and safe manner. The PCE generator policies for active and reactive power obtained for the 5-bus test case, see Section V-A1, are shown in Figure 5 for

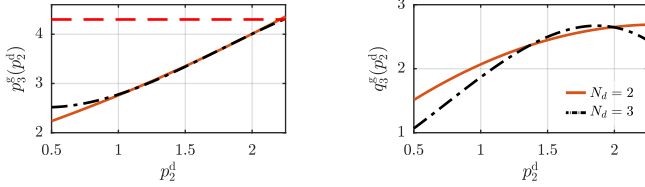


Figure 5. Optimal active/reactive power policies for 5-bus test case.

maximum degrees $N_d \in \{2, 3\}$. The modelled uncertainty follows the Beta distribution from Figure 1b.

We observe that all policies from Figure 5 are non-affine, and that the policies obtained with $N_d = 3$ are more curved. The policies show a significant curvature around $p_2^d = 1.1$ for active power and $p_2^d = 1.7$, for reactive power, which happens to be the point where an inequality constraint becomes binding. Overall, the reactive power policies have higher curvature than the active power policies owing to stronger nonlinear behavior of reactive power. We also observe that the upper generation limit $p_{g,3}^{\max} = 4.3$ can be violated by the policy. However, this will be sufficiently unlikely to happen to not exceed the acceptable chance constraint violation probability.

VI. CONCLUSION AND OUTLOOK

The present paper proposes a tractable reformulation of chance-constrained AC-OPF using polynomial chaos expansion (PCE). PCE allows consideration of the full AC power flow equations, and it facilitates moment-based reformulations of chance constraints. The presented approach requires neither sampling, linearizations nor relaxations. The efficacy of the approach is demonstrated for a 5-bus and a 30-bus system. Our results indicate that a maximum degree $N_d = 2$ for the orthogonal basis provides sufficiently accurate solutions to the AC power flow under uncertainty, at a manageable computational cost.

In future work, we will investigate the connection between PCE-based solutions and established control policies such as AGC, AVR. We would also like to address the question of different cost functions, including e.g., reactive power or risk-averse minimization of cost variance. To address scalability to larger power grids, we will investigate tailored algorithms to solve the reformulated optimization problem by, e.g., exploiting the sparsity of the nonlinear program. Basis-adaptive sparse polynomial chaos should be investigated [33], where, starting from a low-dimensional basis, basis polynomials are added only when they are truly needed. Moreover, the effect of adding higher moments to the reformulated chance constraints could provide better reformulations. It would also be interesting to investigate how polynomial chaos relates to distributionally robust chance constraints, perhaps merging the advantages of both approaches. Finally, N-1 security constraints could be incorporated.

REFERENCES

[1] REN21.2018. *Renewables 2018 Global Status Report*. Tech. rep. 2018.
 [2] B. Stott and O. Alsac. "Optimal Power Flow - A Brief Anatomy". In: *XII SEPOPE*. Rio de Janeiro, Brasil, 2012.

[3] F. Capitanescu et al. "State-of-the-art, challenges, and future trends in security constrained optimal power flow". In: *Electric Power Systems Research* 81.8 (2011), pp. 1731–1741.
 [4] M. Vrakopoulou, K. Margellos, J. Lygeros, and G. Andersson. "Probabilistic Guarantees for the N-1 Security of Systems with Wind Power Generation". In: *Proc. of PMAFS*. 2012, pp. 858–863.
 [5] L. Roald, F. Oldewurtel, T. Krause, and G. Andersson. "Analytical Reformulation of Security Constrained Optimal Power Flow with Probabilistic Constraints". In: *2013 IEEE Grenoble Conference*. June 2013, pp. 1–6.
 [6] D. Bienstock, M. Chertkov, and S. Harnett. "Chance-Constrained Optimal Power Flow: Risk-Aware Network Control under Uncertainty". In: *SIAM Review* 56.3 (2014), pp. 461–495.
 [7] J. Warrington, P. Goulart, S. Marthoz, and M. Morari. "Policy-Based Reserves for Power Systems". In: *IEEE Trans. on Pwr. Sys.* 28.4 (Nov. 2013), pp. 4427–4437.
 [8] T. Mühlpfordt, T. Faulwasser, and V. Hagenmeyer. "A Generalized Framework for Chance-constrained Optimal Power Flow". In: *Sustainable Energy, Grids and Networks* 16 (2018), pp. 231–242.
 [9] M. Vrakopoulou, M. Katsampani, K. Margellos, J. Lygeros, and G. Andersson. "Probabilistic security-constrained AC optimal power flow". In: *PowerTech*. Grenoble, France, June 2013.
 [10] H. Zhang and P. Li. "Probabilistic Analysis for Optimal Power Flow under Uncertainty". English. In: *IET Gen., Trans. & Distr.* 4 (5 May 2010), 553–561(8).
 [11] H. Zhang and P. Li. "Chance Constrained Programming for Optimal Power Flow Under Uncertainty". In: *IEEE Trans. on Pwr. Sys.* 26.4 (Nov. 2011), pp. 2417–2424.
 [12] A. Venzke, L. Halilbasic, U. Markovic, G. Hug, and S. Chatzivasileiadis. "Convex Relaxations of Chance Constrained AC Optimal Power Flow". In: *IEEE Trans. on Pwr. Sys.* 33.3 (May 2018), pp. 2829–2841.
 [13] L. Roald and G. Andersson. "Chance-Constrained AC Optimal Power Flow: Reformulations and Efficient Algorithms". In: *IEEE Trans. on Pwr. Sys.* 33.3 (May 2018), pp. 2906–2918.
 [14] E. Dall'Anese, K. Baker, and T. Summers. "Chance-Constrained AC Optimal Power Flow for Distribution Systems With Renewables". In: *IEEE Trans. on Pwr. Sys.* 32.5 (Sept. 2017), pp. 3427–3438.
 [15] A. Lorca and X. A. Sun. "The Adaptive Robust Multi-Period Alternating Current Optimal Power Flow Problem". In: *IEEE Trans. on Pwr. Sys.* 33.2 (2018), pp. 1993–2003.
 [16] A. Nasri, S. J. Kazempour, A. J. Conejo, and M. Ghandhari. "Network-Constrained AC Unit Commitment Under Uncertainty: A Benders' Decomposition Approach". In: *IEEE Trans. on Pwr. Sys.* 31.1 (Jan. 2016), pp. 412–422.
 [17] R. Louca and E. Bitar. "Robust AC Optimal Power Flow". In: *arXiv:1706.09019* (June 2017).
 [18] D. K. Molzahn and L. Roald. "Towards an AC Optimal Power Flow Algorithm with Robust Feasibility Guarantees". In: *20th Power Systems Computation Conference*. Dublin, 2018.
 [19] C. Duan, W. Fang, L. Jiang, L. Yao, and J. Liu. "Distributionally Robust Chance-Constrained Approximate AC-OPF With Wasserstein Metric". In: *IEEE Trans. on Pwr. Sys.* 33.5 (2018), pp. 4924–4936.
 [20] D. Xiu. *Numerical Methods for Stochastic Computations*. Princeton, New Jersey: Princeton University Press, 2010.
 [21] S. Zymler, D. Kuhn, and B. Rustem. "Distributionally robust joint chance constraints with second-order moment information". In: *Math. Progr.* 137.1 (2013), pp. 167–198.
 [22] T. Mühlpfordt, T. Faulwasser, L. Roald, and V. Hagenmeyer. "Solving Optimal Power Flow with non-Gaussian Uncertainties via Polynomial Chaos Expansion". In: *IEEE Conference on Decision and Control (CDC)*. Dec. 2017, pp. 4490–4496.
 [23] T. Mühlpfordt, T. Faulwasser, and V. Hagenmeyer. "Solving Stochastic AC Power Flow via Polynomial Chaos Expansion". In: *IEEE International Conference on Control Applications*. 2016, pp. 70–76.
 [24] A. Engelmann, T. Mühlpfordt, Y. Jiang, B. Houska, and T. Faulwasser. "Distributed Stochastic AC Optimal Power Flow based on Polynomial Chaos Expansion". In: *IEEE American Control Conference (ACC)*. June 2018, pp. 6188–6193.
 [25] J. Li, N. Ou, G. Lin, and W. Wei. "Compressive Sensing based Stochastic Economic Dispatch with High Penetration Renewables". In: *IEEE Trans. on Pwr. Sys.* (2018), pp. 1–1.
 [26] T.J. Sullivan. *Introduction to Uncertainty Quantification*. 1st ed. Vol. 63. Switzerland: Springer International Publishing, 2015.
 [27] W. Gautschi. "On Generating Orthogonal Polynomials". In: *SIAM Journal on Scientific and Statistical Computing* 3.3 (1982), pp. 289–317.
 [28] L. Roald, F. Oldewurtel, B. Van Parys, and G. Andersson. "Security Constrained Optimal Power Flow with Distributionally Robust Chance Constraints". In: *ArXiv e-prints* (Aug. 2015). 1508.06061.
 [29] G.C. Calafiore and L. El Ghaoui. "On Distributionally Robust Chance-Constrained Linear Programs". In: *J. of Opt. Theory and Appl.* 130.1 (2006), pp. 1–22.
 [30] S. Dasgupta, D.J. Hsu, and N. Verma. "A concentration theorem for projections". In: *22nd Conference on Uncertainty in Artificial Intelligence (UAI)*, 2006.
 [31] F. Oldewurtel, L. Roald, G. Andersson, and C. Tomlin. "Adaptively constrained stochastic model predictive control applied to security constrained optimal power flow". In: *IEEE American Control Conference (ACC)*. 2015.

- [32] R.D. Zimmerman, C.E. Murillo-Sanchez, and R.J. Thomas. "MATPOWER: Steady-State Operations, Planning, and Analysis Tools for Power Systems Research and Education". In: *IEEE Trans. on Pwr. Sys.* 26.1 (Feb. 2011), pp. 12–19.
- [33] G. Blatman and B. Sudret. "Adaptive sparse polynomial chaos expansion based on least angle regression". In: *J. of Comp. Phys.* 230.6 (2011), pp. 2345–2367.